Thermomechanical Responses of Microcracks in a Honeycomb Particulate Filter

Naudiyal, Siddhant; Briceno de Gutierrez, Martha; Greenwood, Richard; Bowen, Paul; Simmons, Mark; Blackburn, Stuart; Stitt, Hugh; Gobby, Darren; Mogalicherla, Aswani

[Link to publication on Research at Birmingham portal](#)

Thermomechanical Responses of Microcracks in a Honeycomb Particulate Filter

Siddhant Naudiyal, Martha Briceno de Gutierrez, Richard Greenwood, Paul Bowen, Mark Simmons, Stuart Blackburn, Hugh Stitt, Darren Gobby, and Aswani Mogalicherla*

Manufacturing honeycomb-structured catalysts require a careful understanding of the microstructure of the solid substrate and its dependence on thermal-processing conditions. Herein, it is the thermal responses of microcracks in an uncoated microcracked aluminum titanate honeycomb catalyst is investigated by analyzing the material's resonance frequency using the high-temperature impulse excitation technique. The resonance frequencies are presented as Young's modulus values to avoid sample size effects. Dynamic Young's modulus measurements show closed-loop hysteresis due to microcracks healing and reopening, causing a reversible response. The hysteresis is further used to understand microcracks' dependence on critical thermal-processing conditions used in a catalyst manufacturing plant, including peak operating temperature (800–1000 °C), dwell period (1–3 h), and heating rates (1–5 °C min^{-1}). Microcracks are observed to have two healing responses: instantaneous and delayed healing. Both responses significantly influence the design of catalyst manufacturing. Complete reopening of microcracks from their healing temperature (1150 °C) is a very time-consuming process (50–60 h). However, it is shown in the analysis that microcrack relaxation is a critical phenomenon that must be considered in quality-controlled environments.

1. Introduction

Grain boundary (GB) microcracks have been the focus of material science, fracture mechanics, rock mechanics, damage mechanics, and civil engineering literature. They often appear in polycrystalline ceramics such as aluminum titanate (AT), mullite, aluminosilicates, and cordierite, which are popular catalyst support materials in emission control systems. The origin of microcracks due to a mismatch in the thermal expansion of distinct phases has been widely discussed in literature.[1–3] Among distinct types of microcracked materials, AT is popular for high-temperature catalytic applications such as particulate filters in vehicle exhaust systems. It is well understood in the literature that microcracks have a thermal response, and these cracks act as thermal stress dampeners.[4–6] Using microcracked materials as catalyst supports is particularly challenging without understanding the dynamics of microcrack healing and the interaction of crack surfaces with secondary phases such as catalyst coatings. In some instances, degradation in strength and fracture toughness of the microcracked materials has been reported due to the linking up of microcracks with advancing prominent crack resulting from thermal stresses at elevated temperatures. It is essential to understand the temperature responses of microcracks because of a strong correlation between the microcrack density with temperature and their subsequent effect on the material's fracture toughness and durability during service.[7]

Quantifying the density of microcracks in the ceramics using direct observations such as scanning electron microscope (SEM) or fluorescence imaging requires tedious statistical treatment.[3,7–12] As a result, indirect quantifying methods based on temperature-dependent Young's modulus, shear modulus, thermal expansion, and thermal diffusivity have become popular.[4,7–11,13–22] Among several techniques, quantifying microcracks using high-temperature Young's modulus measurements is gaining attention because of its direct contribution to the estimating of thermal stresses generated during the catalyst manufacturing process. The hysteresis in the material's Young's modulus in a thermal cycle helps to capture the response of the microcracks to the operating temperatures and several analytical

S. Naudiyal, R. Greenwood, M. Simmons, S. Blackburn
School of Chemical Engineering
University of Birmingham
Edgbaston B15 2TT, UK

M. Briceno de Gutierrez
Johnson Matthey Technology Centre
Blount's Court Road, Sonning Common RG4 9NH, UK

P. Bowen
School of Metallurgy and Materials
University of Birmingham
Edgbaston B15 2TT, UK

H. Stitt, D. Gobby, A. Mogalicherla
Johnson Matthey Technology Centre
Belasis Avenue, Billingham TS23 1LH, UK
E-mail: Aswani.mogalicherla@matthey.com

**ADVANCED
SCIENCE NEWS**

www.advancedsciencenews.com

**ADVANCED
ENGINEERING
MATERIALS**

www.aem-journal.com

expressions are available to quantify microcracks using this information.[8,10,23,24]

Both static and dynamic methods are popular in measuring Young's modulus, depending upon the application. In static test methods such as nanoindentation, four-point bend, and tensile or compressive test, direct strain measurement from applied mechanical stress is demonstrated to be a challenging approach for calculating Young's modulus for porous, brittle microcracked ceramics due to gripping of the sample, limited sample shapes and sizes, and lack of flexibility over the measurement temperature range.[25–27] Therefore, dynamic methods such as ultrasound pulse-echo and sonic resonance/impulse excitation techniques (IETs) have been attempted. These techniques are nondestructive and allow continuous measurements of Young's modulus as a function of temperature.[25] In the present work, IET was applied to measure Young's modulus, which is ideal for highly fragile honeycomb structures having spatial variations in density and porosity.

Dole et al. investigated microcracking in monoclinic hafnium oxide using the sonic resonance method to obtain high-temperature (>1000 °C) Young's modulus measurements and demonstrated success in capturing key microstructural features.[20] Bruno et al. conducted extensive research on microcrack characterization using porous microcracked ceramics.[1,3–8,10,14,23] They also used the sonic resonance method for Young's modulus measurements showing hysteresis as the critical indicator for the presence of microcracks, consistent with earlier investigations.[7,8,23] Similarly, Nickerson used the sonic resonance method for characterizing the dynamic high-temperature Young's modulus of porous ceramic materials including microcracked cordierite. The study presented a reversible path-dependent hysteresis in dynamic Young's modulus to show thermomechanical responses of microcracks in cordierite after being exposed to its material softening temperature (1200 °C).[28] The work of Bruno and co-authors was micromechanics focused, linking the microstructural properties of polycrystalline ceramics such as AT and cordierite to the macroscale properties.[29–31]

Although considerable attention has been given to understanding microcracks using thermomechanical characterization methods, their potential applications and the various thermal process conditions they undergo have often been ignored. Bruno et al. investigated microcrack orientation in porous AT using experimental and modeling approaches.[30] The AT samples were formed using extrusion. However, the effect of critical process parameters on microcrack responses, such as the heating ramp rate, dwell periods, and peak operating temperatures, were neglected. The focus here was again on micromechanics. Bruno et al. used neutron and X-Ray diffraction to measure the lattice expansion of AT; samples were again prepared in-house and fired to 1450 °C at a constant heating rate of 5 °C min^{-1}.[32] Bruno et al. used high-temperature ultrasound spectroscopy to measure Young's modulus of cordierite honeycomb. In this study, four microcracked cordierite samples with varying degrees of porosity were evaluated. However, again the thermal process conditions were kept constant.[23] Similarly, Bruno et al. evaluated the thermal properties of a honeycomb sample produced in-house using low ramp rates of 1 °C min^{-1} and firing temperature of greater than 1450 °C. The study showed hysteresis in the thermal expansion curves without evaluating the effect of heating and cooling rate.[4] The review presented by Bruno and Kachanov showed that their research focuses on micromechanics to predict macroscopic properties like Young's modulus and coefficient of thermal expansion from microstructure-driven predictions.[29] In their review, dynamic Young's modulus dependence on thermal-processing parameters was not discussed. Finally, Bruno and Kachanov did not report the microcrack healing temperature of AT due to being limited by their measurement method. Shyam et al. also investigated the elastic properties of cordierite, however, using a single operating temperature of 1000 °C.[10] Similarly, several other studies, including the investigation conducted by Siebeneck and Hasselman and Chen and Awaji, have been focused on material development rather than process development resulting in the process conditions being neglected.[22,33] These studies provide some critical insights into microcracked materials; however, evaluating the catalyst manufacturing parameters may provide a deeper material understanding to improve product design.

The work conducted by Nickerson is the only study which accounted for the influence of thermal-processing conditions on the dynamic Young's modulus of a microcracked material. Nickerson evaluated the effect of heating rates (0.4–20 °C min^{-1}), dwell periods (0–10 h), and peak operating temperatures (800–1200 °C) on the path-dependent hysteresis of microcracked cordierite. The study limited itself to using the same specimen for investigating each process parameter; the sample was reported to reset to its initial state by heating it to its material softening temperature and cooling it back to room temperature. Several critical observations were made in this study, highlighting that microcrack healing increases with peak operating temperature and dwell periods. However, the influence of the dwell period became less pronounced as the peak operating temperature became closer to the material's softening temperature (1200 °C). Nickerson explained that this was due to the limited potential number of microcrack healing sites on the material at higher peak temperatures. The heating rate analysis showed minor accelerated stiffening at the lowest heat rate (0.4 °C min^{-1}) and delayed stiffening at the highest heating rate (20 °C min^{-1}). Nickerson reported that this was due to microcracked materials' thermally driven kinetic nature resulting from microcracks healing. Furthermore, the study also investigated slow growth kinetics by monitoring the sample's isothermal Young's modulus by introducing a dwell period in the cooling cycle. Nickerson described the relaxation in Young's modulus using a standard exponential decay function. However, this analysis was not conducted at room temperature, where the slow crack growth kinetics may differ.[28]

This study thus aims to understand the effect of thermal-processing conditions applicable to catalyst manufacturing and accelerated catalyst aging on microcrack responses, and elucidate the critical role microcracks play in high-temperature applications, such as catalytic converters. The influence of process conditions such as heating rates (1–5 °C min^{-1}), operating temperatures (800–1300 °C), and dwell periods (1–3 h) on microcracks responses in a commercial uncoated porous microcracked honeycomb-structured AT catalyst is evaluated through dynamic Young's modulus measurements using IET.

2. Results and Discussion

2.1. SEM of Microcracked AT

Figure 1 shows the SEM image of a fresh uncoated AT material. It illustrates that in addition to pores, there are three types of microcracks observed in this material. GB microcracks are present at the interfaces between all the phases in the material. Intragranular microcracks, these are microcracks occurring on individual phases of the material. Intergranular microcracks are microcracks extending across multiple phases across the grain. Each of these microcracks is shown by arrows illustrated in Figure 1. Similar observations of microcracks have been reported in the literature.[1,3,4,7–10]

2.2. Microcrack Response to Peak Operating Temperature

In most of the previous studies, Young's modulus has been studied using a single temperature cycle. However, in catalyst manufacturing, microcracked ceramics experience various peak operating temperatures depending on the type of formulation applied, the synthesis process, and the thermal cycle program. The dynamic behavior of microcracked materials has rarely been studied as a function of peak process temperatures. In this work, dynamic Young's modulus was investigated in the thermal cycles with peak temperatures of 800, 900, and 1000 °C, respectively.

Figure 2 shows the dynamic Young's modulus captured for three thermal cycles, each with varying peak operating temperatures. For these experiments, a constant heat-up rate of 5 °C min^{-1}, a dwell period of 1 h, and a cooling rate of 4 °C min^{-1} were maintained. In all experiments shown in Figure 2, a closed-loop hysteresis was observed in dynamic high-temperature Young's modulus measurement for all test specimens. Young's modulus of the material in the cooling cycle was higher than that in the heating cycle, and this difference between heating and cooling increased with the peak temperature. The size of the hysteresis loop increased as the peak temperature increased from 800 to 1000 °C. An isothermal increase in Young's modulus was observed during the 1 h dwell period for
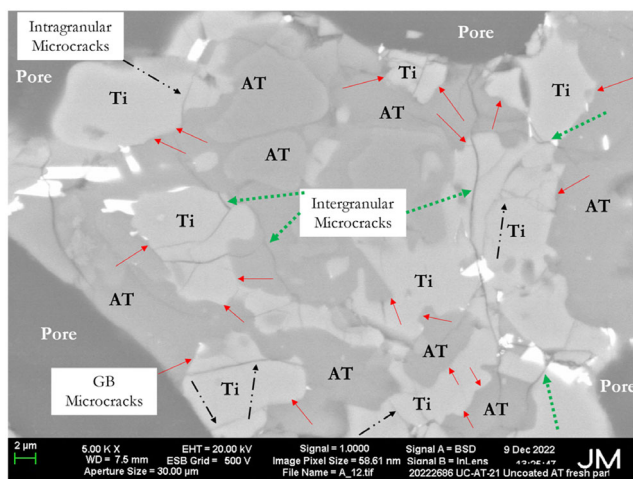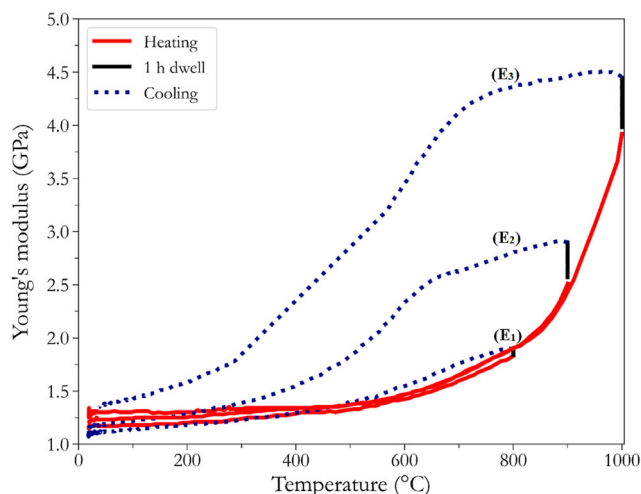

Figure 2. Effect of maximum operating temperature (800–1000 °C) at a constant ramp rate of 5 °C min^{-1}, dwell period of 1 h, and cooling rate of 4 °C min^{-1}.

Figure 1. Scanning electron microscope (SEM) analysis to understand the morphology of microcracked aluminum titanate (AT).

all samples. The effect of 1 h dwell was more pronounced at higher peak temperatures. For all thermal cycles presented in Figure 2, Young's modulus for microcracked AT showed a memory effect resulting in the material returning to its initial state. The apparent Young's modulus was observed to be a function of the temperature program instead of temperature. Multiple Young's modulus values (E_1, E_2, E_3) were observed for the same temperature as illustrated in Figure 2. Similar observations are reported on high-temperature Young's modulus of microcracked materials.[7,20] These observations are also in agreement with the findings of Nickerson, who also reported a reversible path–dependent hysteresis in Young's modulus at similar peak temperatures investigated here, however, for microcracked cordierite.[28]

In Figure 2, there was an increase in the material's Young's modulus upon heating for all samples because of material stiffening resulting from the healing of microcracks. Whereas the reopening of microcracks resulted in material softening, causing a reduction in Young's modulus in the cooling cycle. The differences during healing and opening upon heating and cooling led to hysteresis, which was present for all three operating temperatures. Figure 2 also showed that at higher peak temperatures (1000 °C), Young's modulus does not instantly decrease in the cooling cycle in contrast to low peak temperature (800 °C). A similar result was observed by Nickerson when investigating different peak temperatures.[28] This may be because microcrack healing is stronger at higher peak temperatures (1000 °C) than microcrack healing achieved at 800 or 900 °C, implying microcracks may not open until the thermal tensile forces within the material are sufficient to reopen closed microcracks. The final room-temperature Young's modulus of the samples cooled down from a peak temperatures of 800 and 900 °C was lower than the initial room-temperature Young's modulus of the samples. This implies that the material's microcrack density increased after the thermal cycle in both cases resulting in material softening. In contrast, the specimen exposed to the 1000 °C thermal cycle

**ADVANCED
SCIENCE NEWS**

www.advancedsciencenews.com

**ADVANCED
ENGINEERING
MATERIALS**

www.aem-journal.com

resulted in a higher room-temperature Young's modulus after cooling. This implies a reduction in the material's microcrack density and hence resulting in a stiffer material.

This understanding of the microcrack evolution in AT from Figure 2 about peak process temperatures may hold potential significance for catalyst manufacturers in selecting operating temperatures during the calcination step of microcracked catalyst production. Figure 2 is crucial in showing that catalyst manufacturers need to be cautious in increasing process temperatures because high Young's modulus is observed during cooling which may give rises to additional thermal stresses resulting in increasing likelihood of material cracking during manufacturing.

2.3. Microcrack Response to Thermal Aging

The manufacturing process route for a solid honeycomb catalyst varies significantly depending on the type of coating applied. One of the critical process parameters in catalyst manufacturing is the dwell period, where the coated catalyst is heated to a high temperature and held for a set period to allow the washcoat to adhere to the honeycomb substrate. The manufactured catalyst products are typically subjected to chemical and thermal aging processes. In the aging process, the catalyst is again heated to a high temperature (800–1200 °C) and dwelled for a prolonged period to assess durability and catalytic activity. During the aging process, the catalyst structure/shape changes resulting in reduced catalyst performance due to the elimination of active sites. Although thermal aging test procedures and literature are well established, the response of microcracked materials as a function of dwell periods during aging and manufacturing is currently unknown. Therefore, the effect of the dwell period (1, 2, and 3 h) on microcrack responses in an uncoated AT catalyst was investigated at a constant peak operating temperature of 900 °C.

Figure 3 shows the results of dynamic Young's modulus for these experiments, where the samples were heated to a peak temperature of 900 °C at a constant heating rate of 5 °C min^{-1}, varying dwell period (1, 2, and 3 h) and cooled back to room temperatu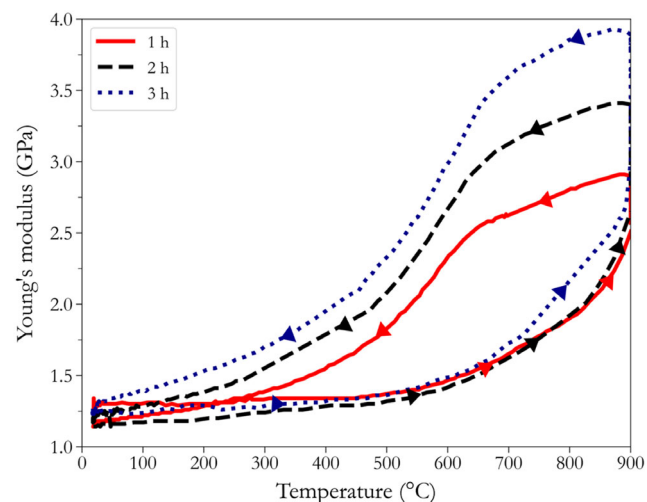re at a fixed cooling rate of 4 °C min^{-1}. Figure 3 again shows that Young's modulus increased with temperature and decreased during cooling resulting in a reversible closed-loop hysteresis for all thermal cycles. The dynamic Young's modulus in the cooling curve is higher than in the heating cycle. It is again due to microcracks healing and opening during heating and cooling and returning to their initial state for all dwell periods investigated. As the dwell period increased, the size of the hysteresis loop also increased, and the highest isothermal increase in Young's modulus was observed for the thermal cycle with a 3 h dwell period. As the duration of the dwell period increased, the isothermal increase observed in Young's modulus at 900 °C was more significant. Upon cooling, Young's modulus decreases for all samples from the highest isothermal Young's modulus value observed for each dwell period. The cooling cycle for all sample varies significantly due to the path dependency of microcrack responses.

In Figure 3, Young's modulus of the samples increased during the dwell periods because microcracks were still healing. A matching observation is made by Nickerson, where the material stiffness continued to increase during the dwell period at a constant peak temperature. Additionally, as the duration of the dwell period increased from 1 to 3 h, the microcrack density decreased further, hence showing more isothermal material stiffening in AT. The observations made in Figure 3 is most probably because the healing of microcracks may consist of two responses, instantaneous and delayed microcrack healing which is a typical behavior of viscoelastic material under applied load. Further investigation is required to understand high-temperature viscoelastic behavior of this material. Overall, result presented in Figure 3 is useful for providing guidelines in optimizing oven settings (airflow rates, cooling rates) when conducting aging studies.

2.4. Microcrack Response to the Heating Rate

Extreme temperature fluctuations due to rapid heating and cooling are common for on-road catalytic converter applications, resulting in the thermal shock failure of components. Porous microcracked ceramics are reported to be better suited for on-road applications than their counterpart in the scientific literature, mainly attributed to the existence of microcracks. However, in catalyst manufacturing, the coating applied to the substrate significantly influences the process heating rate (increased volumetric heat capacity). Although a high heating rate is ideal for maximizing production, it can substantially impact the adhesion of the coating applied to the substrate during the calcination step. Hence, significantly lower heating rates are preferred in the catalyst manufacturing industry primarily to avoid the mechanical degradation of coatings. Therefore, the effect of heating rates 1, 3, and 5 °C min^{-1} has been investigated.

2.4.1. Heating Rates of 3 and 5 °C min^{-1}

Two AT specimens were heated to 900 °C at 3 and 5 °C min^{-1}, respectively, and dwelled for 1 h before being cooled down to room temperature at a constant cooling rate of 4 °C min^{-1}. **Figure 4** shows Young's modulus for two thermal cycles with a varying heating rate of 3 and 5 °C min^{-1}. For both heating rates,

Figure 3. Effect of dwell time (1–3 h) at a constant heating rate of 5 °C min^{-1} and cooling rate of 4 °C min^{-1}.

**ADVANCED
SCIENCE NEWS**

www.advancedsciencenews.com

**ADVANCED
ENGINEERING
MATERIALS**

www.aem-journal.com

Figure 4. Effect of heating rates (3 and 5 °C min^{-1}) on microcracks responses at a constant dwell period of 1 h and cooling rate of 4 °C min^{-1}.

a closed-loop hysteresis was observed in Figure 4. There is a slight variation in the initial room-temperature Young's modulus of both specimens. This slight variation in Young's modulus arises due to the sample being acquired from two different locations in the AT honeycomb substrate. However, overall, the heating cycles were almost identical, showing an insignificant impact of the heating rate.

2.4.2. Heating Rates of 1 and 5 °C min^{-1}

The lowest possible heating rate (1 °C min^{-1}) in the IET furnace was investigated to understand the effect of a low heating rate. However, for this investigation, the experimental run was limited to a peak temperature of 800 °C due to the relatively long run time experienced at 1 °C min^{-1} resulting from heating the sample slowly.

Figure 5 shows the closed-loop hysteresis in Young's modulus for the 1 and 5 °C min^{-1} thermal cycles. Both heating rates
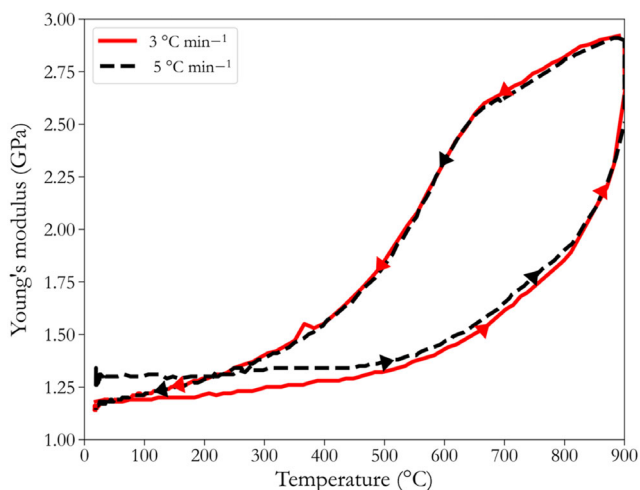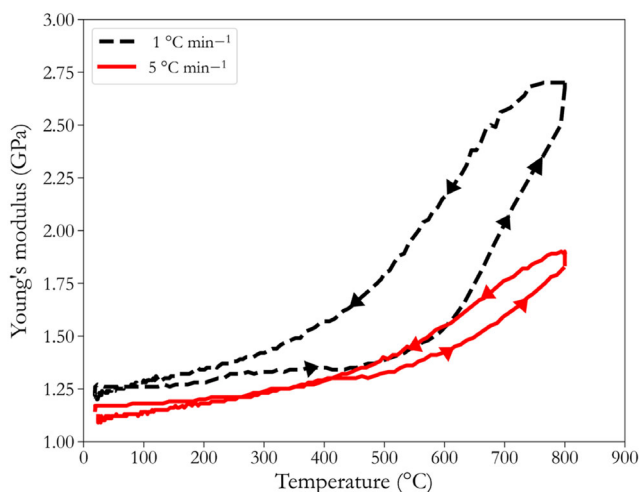

Figure 5. Effect of heating rates (1 and 5 °C min^{-1}) on microcracks responses at a constant dwell period of 1 h and cooling rate of 4 °C min^{-1}.

resulted in a closed-loop hysteresis in the dynamic Young's modulus. However, the size of Young's modulus hysteresis loop for 1 °C min^{-1} was more significant than the one obtained at 5 °C min^{-1}. The Young's modulus profile for both heating rates was initially parallel until around 600 °C. As the temperature increased above 600 °C, the slope of the Young's modulus curve heated at 1 °C min^{-1} was significantly higher than the slope of the curve heated at 5 °C min^{-1}.

For the heating rate experiments shown in Figure 5, that there was a significant difference in the residence time of the two samples. The sample heated at 1 °C min^{-1} took 10 h to reach 600 °C, in contrast to the sample heated at 5 °C min^{-1}, which only took 2 h. This resulted in a significant difference between the closed-loop hysteresis observed at the two heating rates showing that microcrack healing is a thermally activated kinetic process. The delayed microcrack healing response was more pronounced at the lower heating rate. This may be because the potential delayed microcrack healing surfaces have more time to heal when the sample is heated slowly. The healing of these delayed microcrack healing surfaces resulted in further increase in stiffness. The accelerated stiffening at low heating rates and delayed stiffening at high heating rates were also observed by Nickerson; however, the heating rate effect in that study was not as significant.[28] This may be related to the difference in the extent of microcracking in cordierite and AT.

The influence of the heating rate shown in Figure 5 is a significant finding because it illustrates that if microcracked materials are heated rapidly, they portray significantly less change in the material stiffness. It makes them extremely useful for applications where temperature fluctuations are significant and where high heating rates are utilized, such as during soot regeneration of the catalyst. Furthermore, for designing oven shock test procedures, the heating rate is shown to be a significant parameter for microcracked ceramics.

2.5. Thermostability of AT

In a catalyst manufacturing process, the temperature of the catalyst could be significantly higher than the process temperature due to energy released during a reaction, leading to near-miss events or sometimes even resulting in the melting failure of the products. Similarly, melting failure of the catalyst is also a significant challenge for on-road applications in diesel particulate filters during the soot regeneration process, where the occurrence of near-miss events is highly likely. Again microcracked materials like AT are a predominant material choice for this application due to its relatively high melting point. However, the contribution of microcrack responses toward increased thermal durability of the material at temperatures beyond their material softening temperatures still needs to be discovered. Therefore, AT was subjected to a temperature of 1300 °C, and Young's modulus was evaluated to correlate microcrack responses to the material's thermal durability.

Figure 6 shows Young's modulus of the AT in the 1300 °C temperature cycle for two identical samples obtained from the different locations of the same substrate. The observations shown in Figure 1–4 presented a closed-loop reversible hysteresis in Young's modulus. However, in Figure 6, an open-loop
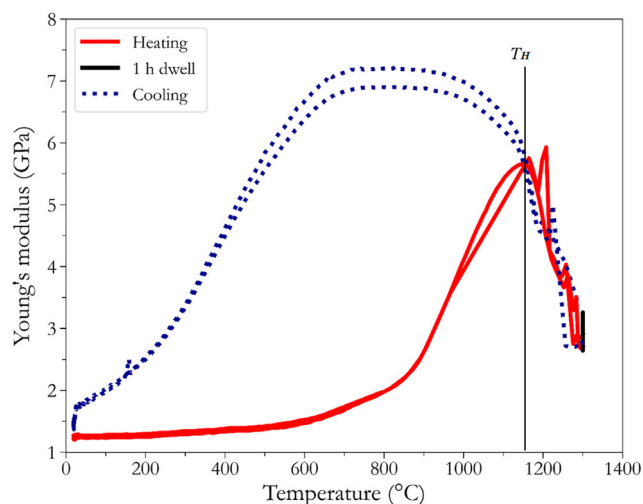
Figure 6. Investigating microcrack healing temperature at a constant ramp rate of 5 °C min⁻¹, dwell period of 1 h, and cooling rate of 4 °C min⁻¹ (data shown for two samples).

hysteresis was observed. For both samples, Young's modulus increased, and accelerated material stiffening occurred at temperatures above 800 °C. In the heating cycle, material stiffness reached maximum point (T_H), this was the material softening temperature (1150 °C). Beyond the point, heating the material resulted in accelerated material softening. The 1 h dwell at 1300 °C resulted in an isothermal increase in Young's modulus. The cooling cycle resulted in accelerated stiffening as the samples cooled down from 1300 °C to T_H and followed a near-identical path to the heating cycle in this temperature range. As the temperature falls below T_H, the material stiffness continues to increase eventually reaching a saturation point. This region is where the highest Young's modulus of the sample was observed. The material stiffness remains constant for few hundred degrees (650–1000 °C). As the temperature decreased below 650 °C, accelerated softening of the material began and continued till room temperature. Finally, in the cooling cycle, a room-temperature isothermal decrease in the samples Young's modulus was observed.

In Figure 6, Young's modulus of the samples increased during heating due to the healing of microcracks. Based on the observations made so far that microcracks heal with heating, observation of the maximum point in the heating cycle, T_H shows that the material softening temperature is 1150 °C. This implies that this could be the complete microcrack healing temperature of the material, where all the potential microcrack healing sites have healed. The material resulted in accelerated softening as the temperature increased from T_H to 1300 °C. This could be because the material behaves like a porous non-microcracked material; hence, microcracking mechanism is no longer dominant in the material. Reduction in the material stiffness during heating is commonly observed for porous non-microcracked materials exposed to high temperatures.[20,28,34,35] Additionally, noise in the dynamic Young's modulus was observed in Figure 6 for both heating and cooling cycles at temperatures greater than T_H due to difficulty in capturing the short-lived sound signal at high

temperatures for this material. Nie et al. reported the same challenge of capturing the resonant frequencies at high temperatures (1300 °C) for determining the dynamic high-temperature Young's modulus of alumina using IET. Nie et al. explained that the vibration signal from the alumina sample became weak at high temperatures and hence could not be detected by the microphones easily.[36] Bruno and Kachanov also reported complications regarding Young's modulus measurements of AT at temperatures higher than 1200 °C due to creep strains.[29] The Young's modulus profile in the cooling cycle followed a near-identical path to Young's modulus profile in the heating cycle as the temperature decreased from 1300 to T_H. Similar observations are reported for the cooling of non-microcracked ceramics from high temperatures.[20,28,34] In the cooling cycle, as the temperature dropped below T_H, there was an increase in material's stiffness. This is still due to the absence of microcracking mechanism in the material. Nickerson reported a similar result during the cooling of microcracked cordierite from 1200 °C and explained that cooling resulted in resetting of the material due to redistribution of microstresses. Nickerson further explained that this mechanism does not occur until the material is exposed to higher temperatures (T_H), which enables additional healing.[28] Upon cooling to the room temperature, the room-temperature Young's modulus was >10% higher than the initial room-temperature Young's modulus. The room-temperature Young's modulus was monitored by introducing a 13 h room-temperature dwell where an isothermal decrease in Young's modulus was observed. This was due to microcracks reopening slowly and is related to slow crack growth kinetics.[28] This phenomenon is known as microcrack relaxation, as even after 13 h the material did not return to its initial state. Studies conducted by Bruno et al. and Dole et al. also reported that Young's modulus of a microcracked material takes a very long time to return to its initial value after heating to high temperatures.[20,23]

Figure 6 highlighted that even when a microcracked material is subjected to severe temperature conditions, it survives and returns near enough to its initial state showing viscoelastic behavior and high-temperature thermal durability. This viscoelastic nature of porous microcracked ceramics makes them ideal candidates for high-temperature applications.

2.6. Microcrack Relaxation

Microcracked honeycomb catalysts are quality tested using various characterization methods immediately after manufacture. Microcracked ceramics exposed to ultrahigh temperatures exhibit time-dependent viscoelastic nature due to multiple mechanisms reported in the literature, such as grain-boundary sliding, diffusion, dislocation, and solution precipitation resulting in stress relaxation.[37] However, AT is polycrystalline material, hence slow growth of microcracks is a likely mechanism in this material class.[28] Microcracked materials have been reported to take an extremely long time to return to their initial state. However, quantitative guidance is yet to be provided to allow accurate post-characterization of catalysts.[23] Hence, microcrack relaxation for honeycomb structures was examined by taking isothermal room-temperature Young's modulus measurements for 25 h. Before capturing the material's response, the two

samples were exposed to the same thermal cycle illustrated in Figure 5. Microcrack relaxation refers to the time taken for the material to return back to its initial room-temperature Young's modulus. As the integrated material control engineering (IMCE) IET furnace cools, at $T \leq 275\,°C$, the cooling rate becomes slower than the defined cooling rate ($4\,°C\,min^{-1}$). However, microcrack relaxation in this study is measured when the furnace has cooled down to room temperature. Additionally, cooling down from $275\,°C$ to room temperature only takes several hours (2–3 h), whereas microcrack relaxation takes place over many hours (50–60 h). In these experiments, thermal equilibrium between the furnace temperature and the sample was maintained using forced convective air supply.

Figure 7 shows normalized isothermal room-temperature Young's modulus measurements of AT after cooling down from $1300\,°C$ as a function of time denoted as F. The normalized term F is defined by Equation (1) where $E_{R,RT}(t)$ is the relaxing Young's modulus of the specimen at room temperature as a function of time, $E_{S,RT}$ the measured value of the Young's modulus at room temperature at the start of the experiment, and $E_{R,RT}(0)$ is the measured value of the room-temperature Young's modulus when the sample returned to room temperature after the experiment. When F tends to 0, the value of $E_{R,RT}(t)$ tends to its initial room-temperature Young's modulus value, $E_{S,RT}$. Therefore, this is when the material is defined to reach its initial state. Figure 7 shows the normalized Young's modulus values for both samples decreased extremely slowly. The reduction in the normalized Young's modulus was relatively more significant in the first 5 h for both samples. After 5 h, the rate of change in the normalized Young's modulus significantly decreased. The Young's modulus data was only recorded for 25 h to avoid damage to the sample through repeated tapping; hence, an exponential decay function was fitted to the 25 h normalized Young's modulus data of the two samples. In Figure 7, F1 and F2 are the exponential decay function fitted to the samples 1 and 2 data, respectively. F1 and F2 take the general form shown by Equation (2) where A is the position and B is the scale
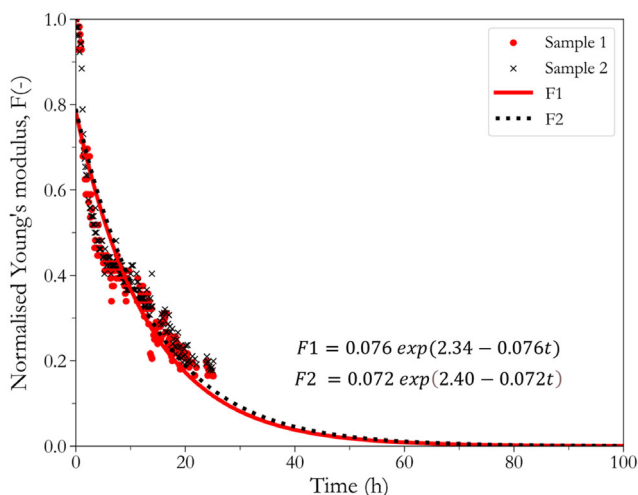
parameter. These equations are showing that the decay functions for both samples are similar and marginal difference arises from the initial difference in the Young's modulus. Using F1 and F2, it was extrapolated that microcracks in AT could take 60 h to relax back to their initial states.

In Figure 7, the normalized Young's modulus values for both samples decreased extremely slowly because the potential microcracks surfaces that healed during the heating cycle were still re-opening and returning back to their initial state. This resulted in slow material softening behavior. This observation is similar to slow crack growth kinetics observed in microcracked cordierite by Nickerson where a 7% reduction in Young's modulus occurred over 9 h during an isothermal dwell in the cooling cycle at $100\,°C$.[28] Exponential decay functions, F1 and F2, showed that it could take the material approximately 60 h to return to its initial state. Dole et al. conducted a similar study on microcracked monoclinic hafnium oxide where relaxation period was as high as 100 h.[20] Bruno et al. has also previously qualitatively described that microcracks return to their initial state after being heated and cooled down from $1200\,°C$ only when they are permitted a "long enough relaxation" period at room temperature. However, the study did not quantify the relaxation period.[23]

Figure 7 highlights that microcracks relaxation is a process that should be considered before conducting any immediate resonance frequency-based characterization on microcracked products after manufacturing, particularly after high-temperature thermal treatment.

$$F = \frac{E_{R,RT}(t) - E_{S,RT}}{E_{R,RT}(0) - E_{S,RT}} \tag{1}$$

$$F1 = \frac{1}{B1} e^{\left(\frac{A1-t}{B1}\right)} \tag{2}$$

3. Conclusion

The hysteresis in the material's stiffness was successfully used as an indirect tool to understand the effect of thermal-processing conditions on microcracks responses in an AT honeycomb catalyst. By mimicking the critical catalyst process-manufacturing conditions, it was observed that microcracked materials such as AT exhibit a strong viscoelastic behavior even when exposed to extreme temperature ($1300\,°C$). This high-temperature durability of AT is primarily attributed to the microcrack responses, essentially acting like thermal stress dampeners that remember and return to their initial state, providing increased thermostability. Additionally, the investigation on process heating rates showed that microcracked ceramics are well suited for rapid heating environments. The influence of heating rate on the dynamic Young's modulus was also significant and revealed that microcracks have two responses; instantaneous and delayed. Just as there is microcrack relaxation in the cooling cycle, where microcracks take an extremely long time to reopen (60 h) even after reaching room temperature, and a similar phenomenon exists during thermal aging. This phenomenon has been referred to as a delayed microcrack healing response in this study. In rapid heating environments such as in a vehicle, delayed microcracks

Figure 7. Determining microcrack relaxation time of AT; isothermal Young's modulus data collected for 25 h after exposing the two samples to the same $1300\,°C$ thermal cycle illustrated in Figure 5.

Plot legend:
- Sample 1
- Sample 2
- F1
- F2

$F1 = 0.076\,exp(2.34 - 0.076t)$
$F2 = 0.072\,exp(2.40 - 0.072t)$

**ADVANCED
SCIENCE NEWS**

www.advancedsciencenews.com

**ADVANCED
ENGINEERING
MATERIALS**

www.aem-journal.com

are not given sufficient time to heal, making them almost resistant to sudden temperature variations. This feature of microcracked materials makes them an excellent choice for high-temperature applications, particularly for on-road emission control technology such as a catalytic converter. The catalyst thermal aging analysis showed that aging time and temperature increase the material stiffness, resulting in higher thermal stresses in the cooling cycle.

4. Experimental Section

IET: High-temperature IET was performed to obtain dynamic Young's modulus measurements in the temperature range (20–1300 °C) using the commercial IET equipment by IMCE Belgium. The experimental setup consisted of a high-temperature furnace (20–1600 °C), a chiller unit for temperature control, and a PC with Resonance Frequency Damping Analyzer (RFDA) data analysis software. Young's dynamic modulus can be determined if the material dimensions, mass, and resonant frequencies are known. Therefore, the specimens were weighed using weighing scales, and the dimensions were measured using Vernier caliper. The flexural frequency required to determine Young's modulus was measured directly through the IET. For this, the sample must be in the flexural mode of vibration. **Figure 8** shows the schematic where the test specimen rested on the alumina nodal tube supports in flexural mode. No standard test methods existed for honeycomb structures for Young's modulus measurement.
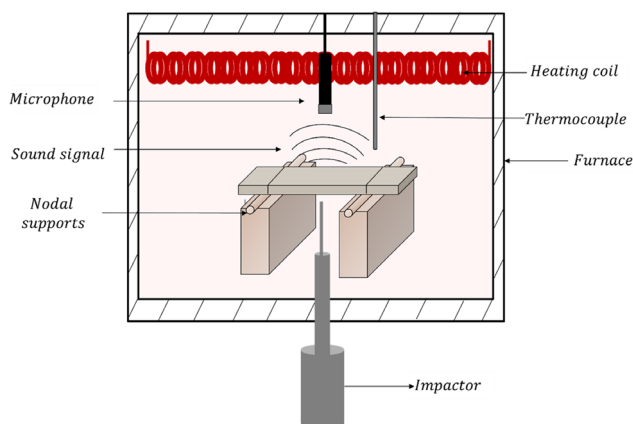

Figure 8. Impulse excitation techniques (IET) experimental setup.

Hence, the E1876 standard was extended to honeycomb structures in this study to determine the dynamic Young's modulus of the material as a function of temperature. In IET, the specimen should be supported at the nodal points (a region with zero displacements) for these measurements. The nodal points were at 0.224* length of the sample from each end, as reported in the E1876 standard for IET.[38] In this study, a small light ceramic cylindrical impactor was used to strike the center of the rectangular sample to excite the structure, emitting a vibrational sound signal captured by the microphone. The captured sound signal was amplified, and a fast-Fourier transform (FFT) algorithm was applied to obtain the fundamental flexural resonant frequency.[39] Cooling water was circulated using the chiller unit to ensure the effective operation of the mic and impacting tool at high temperatures. The dynamic Young's modulus calculation was performed by the RFDA software using Equation (3), where E is Young's modulus (GPa), m is the mass of the bar (g), b is the bar width (mm), L is the bar length (mm), t is the bar thickness(mm), f_f is the fundamental resonance frequency of the bar (Hz), and T_1 is a correction factor.

$$E = 0.9465 \left(\frac{m f_f^2}{b} \right) \left(\frac{L^3}{t^3} \right) T_1 \tag{3}$$

Sample Preparation: The test specimens for Young's modulus measurements were prepared from a commercially available AT-based substrate. The honeycomb cells in this structure were alternately end-plugged to form the inlet and outlet faces of the filter. These plugs (nearly 10 mm deep) were sliced from both ends to obtain a flow-through honeycomb structure, as shown in **Figure 9**. As shown in **Figure 10**a, the honeycomb substrate used in this study used the asymmetric cell technology (ACT) honeycomb design, where a large cell followed a small cell. Figure 10b shows the resulting sample as an Euler beam bar. The specimen dimensions were approximately $100 \times 25 \times 12.5$ mm. Young's modulus measurements at room temperature showed that consistent flexural frequency readings are possible when the width-to-thickness ratio is higher than or equal to 2.

Young's modulus calculated from Equation (1) was extremely sensitive to the specimen dimensions. Hence, to obtain accurate measurements, the specimen was carefully filed using a diamond-cut hand file to achieve a sample free of struts and uneven surfaces resulting from the cutting step. The AT samples produced were highly fragile; hence, careful manual handling during filing was essential to prevent damage and breakage of the specimen. Filing the samples improved the contact between the impactor and specimen surface, resulting in consistent excitations and flexural frequency measurements. The filing operation should be highly gentle to avoid introducing additional damage to the material. Samples damaged during sample preparation or manual handling were discarded from the study. The excitation force of the IET impactor was kept extremely low in this study to prevent indentation through repeated tapping at
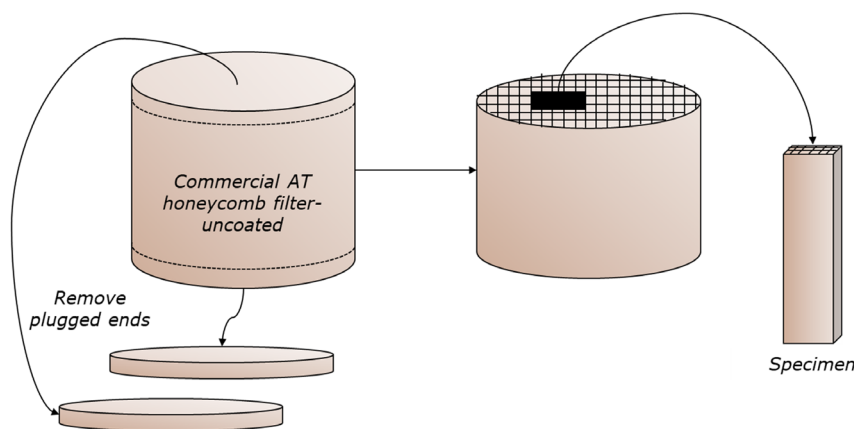

Figure 9. Schematic to show how a rectangular honeycomb specimen is obtained from a cylindrical honeycomb filter.

**ADVANCED
SCIENCE NEWS**

www.advancedsciencenews.com

**ADVANCED
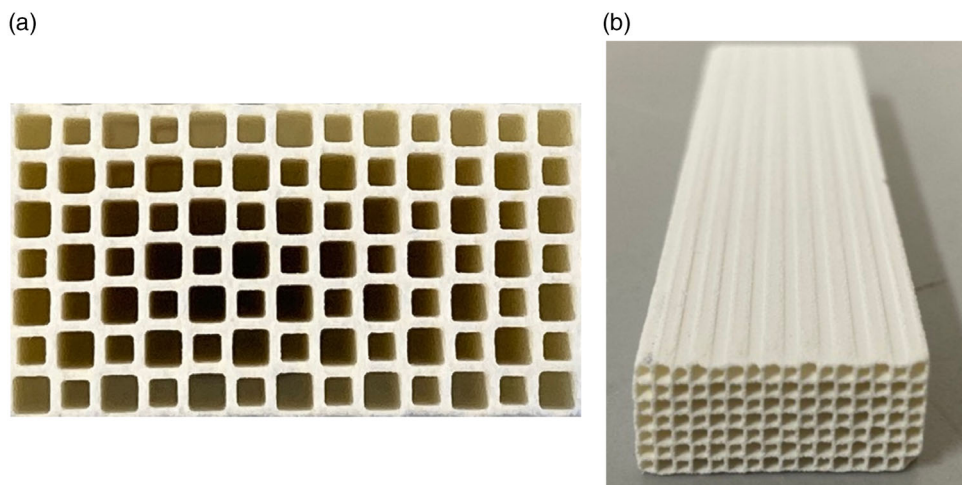ENGINEERING
MATERIALS**

www.aem-journal.com

(a) (b)

Figure 10. a) Asymmetric cell technology (ACT) honeycomb design and b) rectangular honeycomb specimen.

the exact location. The final AT honeycomb specimen was light and tended to move when excited. Hence, utilizing a low-excitation force also ensured that the specimen remained in a flexural mode of vibration throughout the experiment.

The resonance frequency of the sample was captured in 2 min intervals using a sampling rate of $400\,000\,S\,s^{-1}$.

Repeatability of IET: The IET is a robust, versatile technique, rapidly gaining industrial attention for nondestructive applications and characterization of material's mechanical properties. The repeatability of IET was investigated for microcracked honeycomb specimens by obtaining ten rectangular samples from a single uncoated AT honeycomb substrate. The Young's modulus of each sample was measured five times to obtain an average Young's modulus value and the standard deviation. The average Young's modulus range was 1.04–1.30 GPa. The variation in the average room-temperature Young's modulus was due to obtaining the samples from different locations in the AT honeycomb substrate. IET was observed to be a highly repeatable technique for obtaining Young's modulus measurements. Furthermore, the calculated standard deviation of the measurement for all specimens was negligible. For

example, the average Young's modulus of one of the specimens was $1.264\,GPa \pm 0.005$.

Thermal Profile of the IET Furnace: **Figure 11** shows the thermal profile of the IMCE oven where dynamic Young's modulus measurements are conducted. In Figure 11, two thermal profiles are illustrated, one shows IMCE IET oven program defined for a particular experiment. In this instance, a maximum operating temperature of 900 °C, heating rate of $5\,°C\,min^{-1}$, dwell period of 1 h, and cooling rate of $4\,°C\,min^{-1}$ was selected to define a particular thermal cycle. The second thermal profile in Figure 11 illustrates the temperature inside the oven captured by the in-built thermocouple. Figure 11 shows that during the heat-up process and 1 h dwell, there was no significant difference between the temperature measured by the thermocouple and the oven temperature program defined. However, in the cooling cycle, the cooling rate of the oven was only linear until approximately 275 °C. Below this temperature, the cooling rate was slower than $4\,°C\,min^{-1}$. Convective forced air cooling was applied in both heating and cooling cycles to maintain thermal equilibrium between the furnace temperature and the sample.

SEM Analysis of Microcracked at: The samples were analyzed using a Zeiss ultra 55 field-emission electron microscope equipped with in-lens secondary electron and backscattered detectors. For the cross sections, the samples were embedded in resin, ground, polished, and carbon-coated. Energy-dispersive X-ray spectroscopy mapping was used for chemical microanalysis.

The following conditions were used for compositional analysis and low-resolution general imaging: 1) Accelerating voltage: 20 kV 2) Aperture used: 30 µm 3) Working distance: 7.5 mm 4) Detectors: Standard secondary electron and standard backscattered electron detectors.
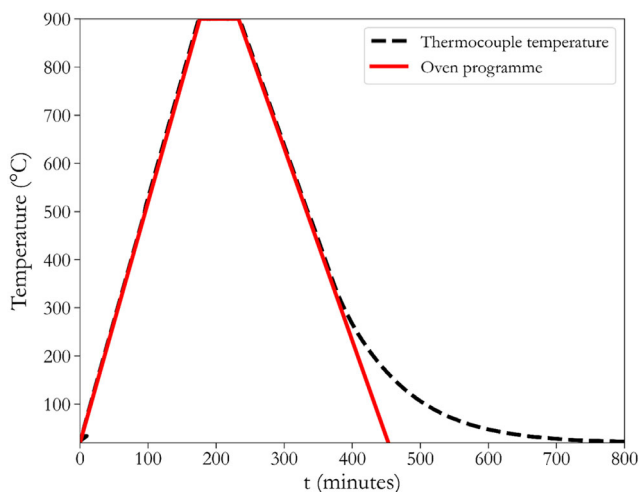
Figure 11. Thermal profile of IMCE IET oven using a constant ramp rate of $5\,°C\,min^{-1}$, dwell period of 1 h, and cooling rate of $4\,°C\,min^{-1}$.

Conflict of Interest

The authors declare no conflict of interest.

Data Availability Statement

The data that support the findings of this study are available from the corresponding author upon reasonable request.

[1] G. Bruno, B. R. Wheaton, B. Clausen, T. Sisneros, *Scr. Mater.* **2013**, *68*, 100.
[2] R. W. Rice, in *Porosity Of Ceramics*, M. Dekker, New York **1998**.
[3] G. Bruno, M. Kachanov, *J. Eur. Ceram. Soc.* **2013**, *33*, 2073.
[4] G. Bruno, Y. Kilali, A. M. Efremov, *J. Eur. Ceram. Soc.* **2013**, *33*, 211.
[5] I. Pozdnyakova, G. Bruno, A. M. Efremov, B. Clausen, D. Hughes, *Adv. Eng. Mater.* **2009**, *11*, 1023.
[6] A. Shyam, E. Lara-Curzio, T. R. Watkins, R. J. Parten, *J. Am. Ceram. Soc.* **2008**, *91*, 1995.
[7] A. Shyam, G. Bruno, T. R. Watkins, A. Pandey, E. Lara-Curzio, C. M. Parish, R. J. Stafford, *J. Am. Ceram. Soc.* **2015**, *35*, 4557.
[8] G. Bruno, M. Kachanov, *J. Eur. Ceram. Soc.* **2013**, *33*, 1995.
[9] D. P. H. Hasselman, K. Y. Donaldson, E. M. Anderson, T. A. Johnson, *J. Am. Ceram. Soc.* **1993**, *76*, 2180.
[10] A. Shyam, E. Lara-Curzio, A. Pandey, T. R. Watkins, K. L. More, *J. Am. Ceram. Soc.* **2012**, *95*, 1682.
[11] O. Alm, L. L. Jaktlund, K. Shaoquan, *Phys. Earth Planet. Interiors* **1985**, *40*, 161.
[12] J. Bisschop, J. G. M. v. Mier, *Heron* **1999**, *44*, 245.
[13] F. C. S. Carvalho, C. N. Chen, J. F. Labuz, *Int. J. Rock Mech. Mining Sci.* **1997**, *34*, 43.e1.
[14] G. Bruno, A. Efremov, C. An, S. Nickerson, *Sci. Proc.* **2011**, *32*, 137.
[15] F. J. Parker, R. W. Rice, *J. Am. Ceram. Soc.* **1989**, *72*, 2364.
[16] E. Eberhardt, B. Stimpson, D. Stead, *Rock Mech. Rock Eng.* **1999**, *32*, 81.
[17] K. Hamano, Y. Ohya, Z. E. Nakagawa, *Int. J. High Technol. Ceram.* **1985**, *1*, 129.
[18] H. C. Kim, K. S. Lee, O. S. Kweon, C. G. Aneziris, I. J. Kim, *J. Eur. Ceram. Soc.* **2007**, *27*, 1431.
[19] D. R. Clarke, D. J. Green, in *Advances in Materials Characterization* (Eds: D. R. Rossington, R. A. Condrate, R. L. Snyder), Springer US, Boston, MA **1983**, p. 323.
[20] S. L. Dole, O. Hunter Jr, F. W. Calderwood, D. J. Bray, *J. Am. Ceram. Soc.* **1978**, *61*, 486.
[21] W. R. Manning, O. Hunter Jr, F. W. Calderwood, D. W. Stacy, *J. Am. Ceram. Soc.* **1972**, *55*, 342.
[22] H. J. Siebeneck, D. P. H. Hasselman, J. J. Cleveland, R. C. Bradt, *J. Am. Ceram. Soc.* **1976**, *59*, 241.
[23] G. Bruno, A. M. Efremov, C. P. An, B. R. Wheaton, D. J. Hughes, *J. Mater. Sci.* **2012**, *47*, 3674.
[24] I. Štubňa, A. Trník, L. Vozár, *Ceram. Int.* **2007**, *33*, 1287.
[25] M. Radovic, E. Lara-Curzio, L. Riester, *Mater. Sci. Eng. A* **2004**, *368*, 56.
[26] S. J. Wu, P. C. Chin, H. Liu, *Appl. Sci.* **2019**, *9*, 2067.
[27] A. Pandey, A. Shyam, T. R. Watkins, E. Lara-Curzio, R. J. Stafford, K. J. Hemker, *J. Am. Ceram. Soc.* **2014**, *97*, 899.
[28] S. Nickerson. *Ph.D. Thesis*, Bauhaus University, Weimar, Germany **2019**.
[29] G. Bruno, M. Kachanov, *J. Am. Ceram. Soc.* **2016**, *99*, 3829.
[30] G. Bruno, A. M. Efremov, B. R. Wheaton, J. E. Webb, *Acta Mater.* **2010**, *58*, 6649.
[31] G. Bruno, S. Vogel, *J. Am. Ceram. Soc.* **2008**, *91*, 2646.
[32] G. Bruno, A. Efremov, B. Wheaton, I. Bobrikov, V. G. Simkin, S. Misture, *J. Eur. Ceram. Soc.* **2010**, *30*, 2555.
[33] C. H. Chen, H. Awaji, *J. Eur. Ceram. Soc.* **2007**, *27*, 13.
[34] W. Pabst, E. Gregorová, M. Černý, *J. Eur. Ceram. Soc.* **2013**, *33*, 3085.
[35] B. A. Latella, T. Liu, *J. Am. Ceram. Soc.* **2005**, *88*, 773.
[36] G. Nie, Y. W. Bao, D. Wan, Y. Tian, *Key Eng. Mater.* **2018**, *768*, 24.
[37] M. Sakai, H. Muto, M. Haga, *J. Am. Ceram. Soc.* **1999**, *82*, 169.
[38] ASTM E1875-08, ASTM International, **2009**, https://doi.org/10.1520/e1875-08.
[39] G. Roebben, B. Bollen, A. Brebels, J. Humbeeck, O. Van der Biest, *Rev. Sci. Instrum.* **1997**, *68*, 4511.